RESEARCH ARTICLE | JUNE 27 2024

Exceptional thermal conductivity increase of Nafion by hydrogen-bonded water molecules *⊙*

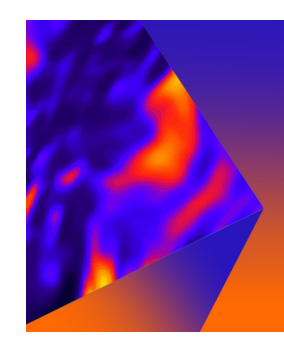
Mahya Rahbar ⊚ ; Qusai Alahmad ⊚ ; John Bai; Lijun Zhang 🕶 ⊚ ; Xinwei Wang 🗷 ⊚



Appl. Phys. Lett. 124, 262202 (2024) https://doi.org/10.1063/5.0217244







Applied Physics Letters

Special Topic: Mid and Long Wavelength Infrared Photonics, Materials, and Devices

Submit Today





Exceptional thermal conductivity increase of Nafion by hydrogen-bonded water molecules

Cite as: Appl. Phys. Lett. 124, 262202 (2024); doi: 10.1063/5.0217244 Submitted: 3 May 2024 · Accepted: 17 June 2024 ·







Published Online: 27 June 2024

Mahya Rahbar, no Qusai Alahmad, no John Bai, Lijun Zhang, no and Xinwei Wang no Mahya Rahbar, no Qusai Alahmad, no John Bai, Lijun Zhang, no Alah Mahya Rahbar, no Qusai Alahmad, no John Bai, Lijun Zhang, no Qusai Alahmad, no John Bai, Lijun Zhang, no Qusai Alahmad, no John Bai, Lijun Zhang, no Qusai Alahmad, no Qusai





AFFILIATIONS

Department of Mechanical Engineering, Iowa State University, Ames, Iowa 50011, USA

ABSTRACT

Nafion, a widely used proton exchange membrane in fuel cells, is a representative perfluorosulfonic acid membrane consisting of a hydrophobic Teflon backbone and hydrophilic sulfonic acid side chains. Its thermal conductivity (k) is critical to fuel cell's thermal management. During fuel cell operation, water molecules inevitably enter Nafion and could strongly affect its k. In this work, we measure the k of Nafion of different water content (λ). Findings reveal that k is significantly low in a vacuum environment characterized as $0.110 \,\mathrm{W\,m^{-1}\,K^{-1}}$, but at $\lambda \sim 1$, a notable increase is observed, reaching $0.162 \,\mathrm{W\,m^{-1}\,K^{-1}}$. Moreover, k at $\lambda \approx 6$ is 60% higher than that of $\lambda \sim 1$. This exceptional k increase is far beyond the theoretical prediction by the effective medium theory that only considers simply physical mixing. Rather this k increase is attributed to the formation of water clusters and channels with increased λ , creating thermal pathways through hydrogen bonding, thereby improving chemical connections within the Nafion structure and augmenting its k. Furthermore, it is observed that Nafion's k reaches the maximum value of 0.256 W m⁻¹ K⁻¹ at $\lambda \approx 6$, with no further increase up to $\lambda \approx 10.5$. This phenomenon is explained by the coalescence of water clusters at $\lambda \approx 6$, forming channels that optimize heat transfer pathways and connections within the Nafion structure. Moreover, the free movement of water molecules within water channels ($\lambda > 6$) shows physical alterations in Nafion structure (significant volume increase), which have a lesser impact on k.

Published under an exclusive license by AIP Publishing. https://doi.org/10.1063/5.0217244

Proton exchange membrane (PEM) fuel cells are recognized as environment-friendly energy solutions applicable in portable, stationary, and automotive settings. Developing PEMs with enhanced performance, stability, and longevity is crucial. These materials should demonstrate superior proton conductivity and robust thermal and chemical durability. 1,2 Nafion, a widely used PEM in fuel cells, is a representative perfluorosulfonic acid membrane consisting of a hydrophobic Teflon backbone and hydrophilic sulfonic acid side chains.³ Understanding the temperature distribution in fuel cells is crucial for efficient thermal management. Nafion's thermal conductivity, strongly influenced by its water content, significantly impacts fuel cell thermal performance.^{4–6} Thus, understanding the thermal conductivity and water content relationship in Nafion is essential for effective thermal management in fuel cells. It is crucial to understand Nafion's ability to maintain optimal hydration levels to design systems that efficiently regulate temperature, preventing overheating, inefficient operation, drying, or flooding, thereby ensuring fuel cell efficiency and durability.

To date, several studies have been conducted to determine the Nafion's thermal conductivity in dry and hydrated states. Khandelwal and Mench⁵ reported the out-of-plane thermal conductivity of dry Nafion [equivalent weight (EW) = 1100 g mol⁻¹] at different temperatures, ranging from $0.16\,\mathrm{W\,m^{-1}\,K^{-1}}$ at room temperature (RT) to $0.13 \,\mathrm{W\,m^{-1}\,K^{-1}}$ at 65 °C. Using the volume average method, they also theoretically estimated the thermal conductivity of hydrated Nafion as 0.30 W m⁻¹ K⁻¹ at 100% relative humidity (RH). Since water content and Nafion are not in parallel configuration in the heat transfer direction, such estimation lacks sound physical base. Burheim et al.4 conducted the ex-site experiment for measuring the Nafion's thermal conductivity as a function of water content. They found the thermal conductivity of dry and fully hydrated Nafion at 20 °C and 4.6 bars compaction pressure as 0.177 and 0.254 W m⁻¹ K⁻¹, respectively. Alhazmi⁶ theoretically estimated the thermal conductivity of hydrated Nafion 115 at various temperatures, considering the humidified membrane as a physical mixing of water and membrane material. The findings indicated a thermal conductivity of 0.188 W m⁻¹ K⁻¹ for dry

²College of Engineering Science and Technology, Shanghai Ocean University, 999 Huchenghuan Road, Shanghai 201306, People's Republic of China

^{a)}Authors to whom correspondence should be addressed: ljzhang@shou.edu.cn and xwang3@iastate.edu

Nafion and an increased value of 0.400 W m⁻¹ K⁻¹ at 100% RH at 35 °C. Vie and Kjelstrup⁸ determined the thermal conductivity of fully hydrated Nafion 115 by evaluating the parallel structure of polymer and water, yielding a value of 0.18 W m⁻¹ K⁻¹. Burford and Mench⁹ provided an estimation for the thermal conductivity of Nafion 111 in the range of 0.025–0.25 W m⁻¹ K⁻¹, utilizing embedded microthermocouple in the electrolyte with significant uncertainty. Chen et al.10 measured the thermal conductivity of dry Nafion 117 as 0.14 W m⁻¹ K⁻¹, supplementing their findings with predictions based on non-equilibrium molecular dynamics (MD) simulations at varied water contents and temperatures. Zheng et al. 11 employed MD simulations to determine the thermal conductivity of hydrated Nafion, reporting a value of 0.24 W m⁻¹ K⁻¹ at 300 K. Alhazmi et al. reported the in-plane and out-of-plane thermal conductivity in different temperatures. Their results were $0.188\,\mathrm{W\,m^{-1}\,K^{-1}}$ for in-plane 12 and $0.193 \,\mathrm{W \, m^{-1} \, K^{-1}}$ for out-of-plane directions ¹³ at 35 °C. The small difference in thermal conductivity between these two directions suggests an isotropic structure for Nafion.1

Despite these studies contributing significantly to advancements in understanding Nafion's thermal conductivity, direct measurement of the thermal conductivity of Nafion under different RH and comprehensive physics-based explanation regarding the enhancement of thermal conductivity with increased water content remain a notable gap. In this study, the out-of-plane thermal conductivity of a Nafion is measured under various hydration levels, up to 94% RH, along with the thermal conductivity of dry Nafion in a vacuum environment for comparison purposes, using the differential thermal resistance (DTR) technique. Additionally, the in-plane thermal conductivity of dry Nafion in vacuum is determined using the transient electro-thermal (TET) technique, aiming to evaluate the isotropic structure of our sample. We elucidate the impact of water molecules on the Nafion polymer structure and provide an explanation on how it influences thermal conductivity through the formation of hydrogen bonding.

In this study, we investigate the Nafion 117 from Ion Power, Inc., with a measured thickness of 181 $\mu \rm m$ using a digital micrometer. The density (ρ) of the membrane is determined to be 1994 kg m $^{-3}$ by directly measuring its mass and volume at RT and a specified RH of 16%. To further understand the thermal properties of the material, the specific heat capacity (c_p) of the sample is determined to be 1370 J kg $^{-1}$ K $^{-1}$ using differential scanning calorimetry at 20 °C. This value will be later used in the in-plane thermal conductivity calculation.

The water content (λ) serves as a crucial parameter for the molecule-based comparison of membrane hygroscopic properties. 16 In Fig. 1(a), the relationship between the number of water molecules per sulfonic acid group ($\lambda = n_{\rm H_2O}/n_{\rm SO_3H}$) and RH is illustrated, which is obtained from dynamic vapor sorption measurements by having the membrane in contact with water vapor at 25 °C. 15 The plot indicates an increase in λ with rising RH. The density of hydrated Nafion holds significant importance for determining the volume fraction of water and Nafion components, which will be elaborated in the supplementary material through the use of effective medium theories. The left axis of Fig. 1(b) presents the effective density of Nafion at different water contents, as measured by Bai et al. 16 The density exhibits an initial slight increase followed by a decrease as water content rises. At low water contents, water molecules occupy free spaces within the Nafion structure, and the Nafion polymer volume remains unswollen. Consequently, the mass of hydrated Nafion increases without a volume expansion, leading to an increase in density. However, higher water contents cause the Nafion polymer to expand, resulting in an overall decrease in density.¹⁰ The right axis of Fig. 1(b) displays the swelling ratio of Nafion 117, as reported by Feng et al.¹⁷ Swelling ratio represents the volume difference of Nafion before and after water absorption, relative to the initial Nafion sample volume. It is evident that at lower water contents, the swelling ratio remains minimal. However, as water content surpasses approximately $\lambda \approx 6$, the swelling ratio increases significantly, causing Nafion to swell and reduce its density. Bai et al. 16 reported a density of approximately 2043 kg m $^{-3}$ at \sim 16% RH, which is in good agreement with our result of 1994 kg m⁻³. Therefore, we use their reported density for different water contents in our data processing.

The DTR technique is used to measure the out-of-plane thermal conductivity of Nafion. Additional details and experimental data are available in the supplementary material. The out-of-plane thermal conductivity of Nafion in atmospheric air (16% RH) and vacuum condition, with an uncertainty of 1.67%, is measured to be 0.162 and 0.110 W m⁻¹ K⁻¹, respectively. This decrease in thermal conductivity in the vacuum environment is attributed to the significantly lower RH compared with atmospheric conditions. Moreover, as shown in Fig. 2(a), the thermal conductivity of Nafion at \sim 70% is 1.6 times that at 16%. Then, it remains pretty much constant until reaching full hydration. The physics behind this behavior will be explained later in the paper. To date, several researchers have estimated the thermal conductivity of hydrated Nafion. Khandelwal and Mench⁵ reported the theoretical thermal conductivity of Nafion (EW = 1100 g mol⁻¹) using

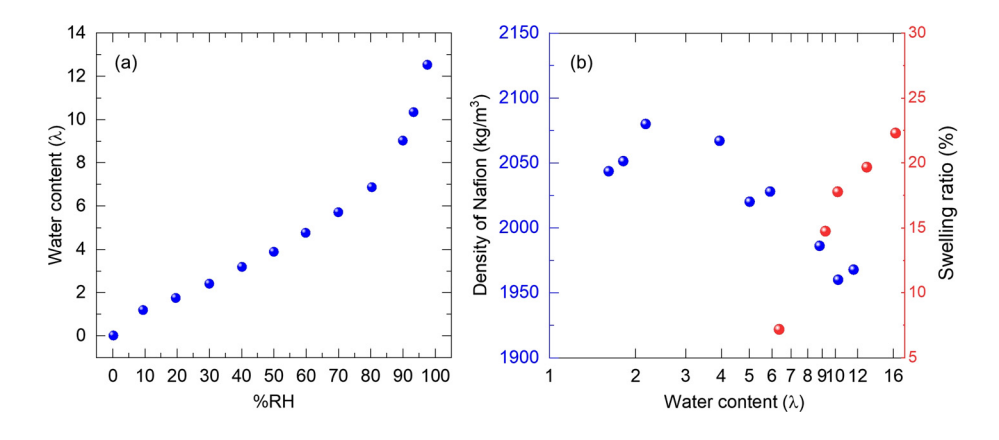


FIG. 1. (a) Water content as a function of RH. ¹⁵ (b) The density ¹⁶ (blue dots) and swelling ratio (red dots) of Nafion 117 ¹⁷ at different water contents.

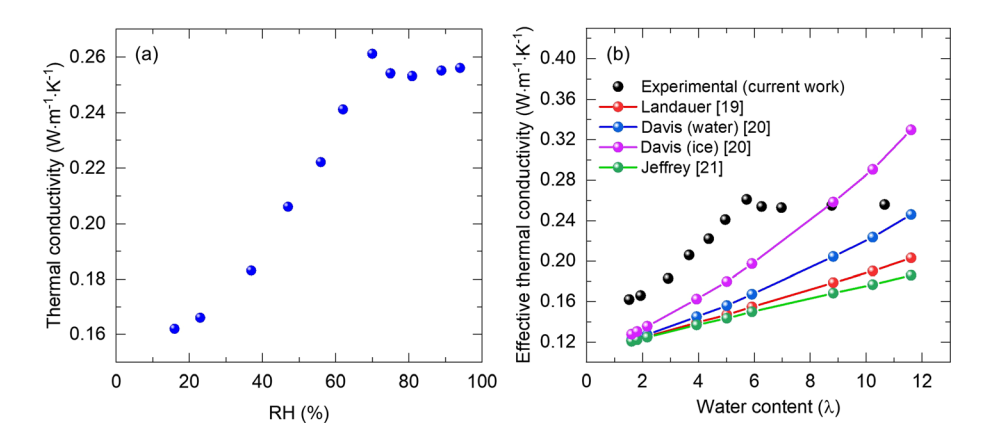


FIG. 2. (a) Measured out-of-plane thermal conductivity as a function of RH. (b) Experimental out-of-plane thermal conductivity as a function of water content in comparison with the prediction using different effective medium theories. ^{19–21}

volume averaging at different RHs and temperatures. This physical treatment is not appropriate as the water molecules and Nafion are not parallel in the heat transfer direction. Burheim et al.4 measured the thermal conductivity of Nafion at 20 °C and 4.6 bars compaction pressure. Their result is 0.177 W m⁻¹ K⁻¹ for dry Nafion and 0.254 W m⁻¹ K⁻¹ at 100% RH, exhibiting a strong agreement with the results obtained in this study. They demonstrated the incompressibility of Nafion by measuring the thickness of the sample with and without applying pressure in the range of 0.5-10 bars, revealing no signs of compressibility. Chen et al.¹⁰ reported the thermal conductivity of dry Nafion as $0.14 \,\mathrm{W\,m^{-1}\,K^{-1}}$, exhibiting good agreement with our obtained value of $0.11 \,\mathrm{W\,m^{-1}\,K^{-1}}$. Alhazmi⁶ calculated the effective thermal conductivity of the hydrated Nafion 115 by averaging the thermal conductivity of the water, air, and Nafion considering their volume fractions at different temperatures, assuming that the humidified membrane behaves as a mixture of water and membrane material. They also measured the thermal conductivity of dry Nafion using a conventional steady states technique at different temperatures. Their result showed the thermal conductivity of 0.188 W m⁻¹ K⁻¹ for dry Nafion and 0.400 W m⁻¹ K⁻¹ at 100% humidity at 35 °C. The discrepancy observed could be attributed to the experimental temperature in Alhazmi's work,6 which is 35 °C, while we conducted our measurements at RT. It is important to note that the thermal conductivities of water and Nafion tend to increase with increased temperatures. 19

Additionally, we present Nafion's in-plane thermal conductivity, measured using the TET technique, compare it with out-of-plane thermal conductivity results, and understand the structure of Nafion. The in-plane thermal conductivity is determined to be $0.112\,\mathrm{W\,m^{-1}\,K^{-1}}$, which is very close to the out-of-plane thermal conductivity of $0.110\,\mathrm{W\,m^{-1}\,K^{-1}}$ in vacuum. This confirms our Nafion sample's good isotropic structure. Our finding aligns with Burheim's conclusion, confirming the absence of any particular orientation in its polymer structure. Additional details and experimental data of TET measurements are available in the supplementary material.

Figure 2(b) presents the experimental results between thermal conductivity and water content, by converting RH to water content using the data in the work of Peron *et al.*¹⁵ Moreover, Fig. 2(b) shows the effective thermal conductivity, as determined by different effective medium theories. More information on these theories can be found in the supplementary material. Effective medium theories need the data of the thermal conductivity of water and intrinsic thermal conductivity of

dry Nafion. Using the thermal conductivity of liquid water as $0.6\,W\,m^{-1}\,K^{-1}$ (Ref. 22) at RT and the thermal conductivity of dry Nafion as $0.110 \,\mathrm{W\,m^{-1}\,K^{-1}}$, it is evident that none of the effective medium theories can adequately account for the observed upward trend of thermal conductivity increase with RH, and the experimental thermal conductivity mostly is much higher than the theoretical predictions. Additionally, the effective medium theories are not able to predict the saturation of thermal conductivity at higher water contents. A comprehensive explanation regarding the factors that contribute to the observed saturation in thermal conductivity will be presented later in the paper. Acknowledging the limited mobility of water in the Nafion polymer, if we assume that the water content has a thermal conductivity of ice [2.22 W m⁻¹ K⁻¹ (Ref. 23)], Fig. 2(b) also shows the prediction using the Davis model. Despite the improvement of the results at higher water contents, it is not enough to comprehensively explain the observed experimental results. The observed discrepancy in thermal conductivity could be attributed to the complex chemical structure and bonding interactions between the Nafion polymer and water molecules inside the cavities of polymer, as effective medium theories only consider the physical addition of water within a medium.

In this paragraph, the trend of thermal conductivity increase with water content is elucidated through the exploration of the molecular structures of Nafion and water, as shown in Fig. 3. Adding water to Nafion changes its structure. Initially, as water molecules permeate the pores within Nafion, they increase the connections between polymer chains, leading to more heat conduction channels, thereby increasing Nafion's thermal conductivity. By further increasing the water content, the effect of hydrogen bonds strengthening dominates the formation of additional bonds and increases thermal conductivity. More detailed explanations regarding these mechanisms are provided in the following paragraphs.

When the water content is low ($\lambda \approx 1, 2$), as illustrated in Fig. 3(a), the water molecules induce the dissociation of H^+ from sulfonic acid groups, resulting in the formation of hydronium ions (H_3O^+). Concurrently, water molecules begin to occupy pores within the Nafion membrane. With a gradual rise in water content ($\lambda \approx 5, 6$), as shown in Fig. 3(b), the water molecules further permeate the pores, leading to the swelling of Nafion and the water clusters formation within the Nafion structure. In other words, the Nafion backbone, characterized by its hydrophobic properties, and the sulfonic acid groups, showcasing hydrophilicity, tend to create two distinct environments: water clusters

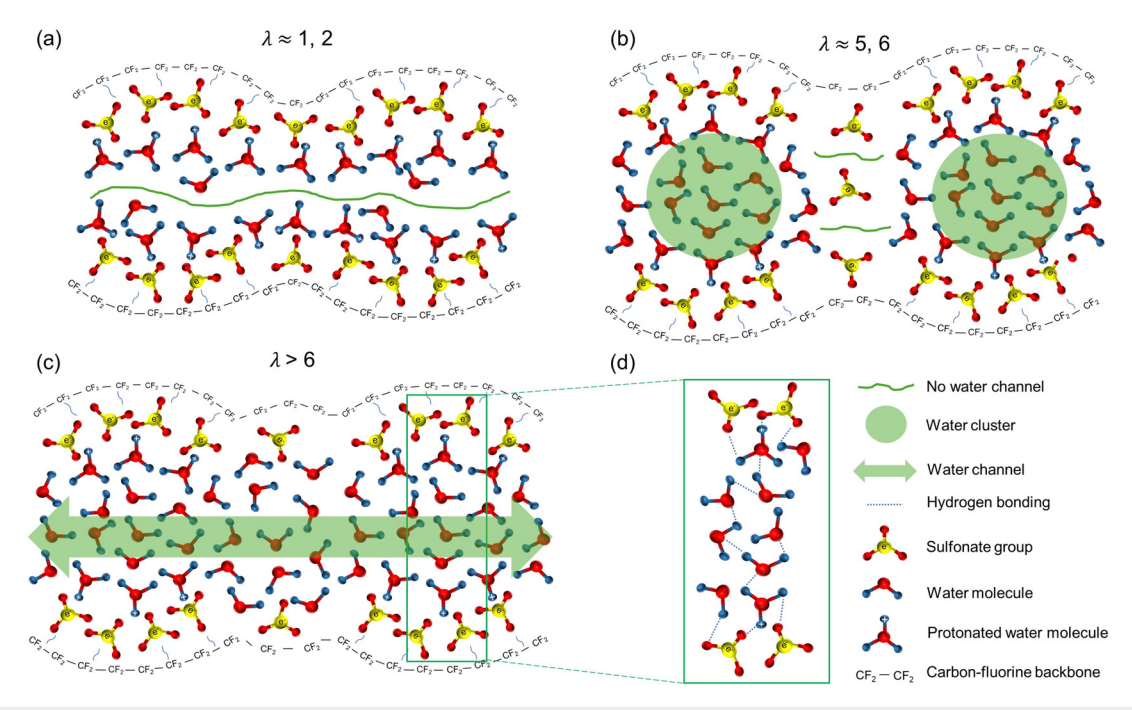


FIG. 3. Schematic of Nafion membrane and water molecules. (a) At low water content levels around $\lambda \approx 1, 2$, sulfonate groups (SO₃⁻) and hydronium ions (H₃O⁺) are generated. At this stage, there is no formation of a water pathway. (b) At the medium water content levels around $\lambda \approx 5, 6$, water clusters with an approximate diameter of 4 nm form. However, these clusters remain disconnected. (c) At higher water content levels of $\lambda > 6$, water clusters coalesce to form channels with an approximate diameter of 1 nm. (d) In these clusters and channels, water molecules form a hydrogen bond network with themselves and/or sulfonate groups. The colors are interpreted as follows: red for oxygen atoms, yellow for sulfur atoms, and blue for hydrogen atoms.

and the polymer matrix. A Note that there is an absence of continuity between clusters at this level of water content. Increasing the water content up to $\lambda \approx 6$ improves the connections between molecules within the sample, thereby enhancing Nafion's thermal conductivity, as shown in Fig. 2(b). In other words, the presence of hydrogen bonding in polymers can facilitate the improvement of existing thermal pathways and potentially create extra pathways, resulting in more effective conduction of heat with reduced phonon scattering. A Zhang et al. Conducted a study on the effect of hydrogen bond density on nanoscale thermal transport in crystalline nylon. Their findings suggest that using the effect of hydrogen bonds can be a suitable approach to enhance thermal conductivity of crystalline polymers.

As shown in Fig. 3(c), at higher water contents ($\lambda > 6$), the clusters coalesce, causing the membrane to be fully extended with channels of water molecules. According to the cluster model proposed by Gierke *et al.*, ^{26,27} clusters featuring a diameter of 4 nm are interconnected via channels with a diameter of 1 nm. In the study by Komarov *et al.*, ²⁴ the estimated characteristic size of water channels varied between 2.5 and 5.0 nm, depending on the water content. As illustrated in Fig. 2(b), increasing water content beyond $\lambda \approx 6$ does not result in further increases in thermal conductivity. This phenomenon can be attributed to the formation of water channels, which create a heat transfer path. Once the channels are established at $\lambda \approx 6$, the thermal conductivity reaches its maximum value, as this configuration provides optimal connections between molecules within the Nafion membrane, forming an optimized heat transfer pathway. In other words, by increasing the water

content up to $\lambda \sim 6$, $\mathrm{H_3O^+}$ ions and water molecules begin to occupy the pores and create hydrogen bonding, impeding their free movement. These chemical alterations in the Nafion structure significantly elevate the thermal conductivity compared with that when $\lambda > 6$. When $\lambda > 6$, water channels form, which allow the unimpeded movement of water molecules and causing Nafion to swell, as shown in Fig. 1(b). Consequently, the changes in thermal conductivity become negligible, as the structural modifications in Nafion primarily occur at a physical level. Mehra *et al.* ²⁸ also reported 1.6 times thermal conductivity enhancement for PVA-PEG polymer compared to pure PVA due to the formation of thermal bridge through hydrogen bonding. The presence of this thermal bridge facilitates phonon transport without scattering.

Nishiyama *et al.*² investigated various chemical states of water within the Nafion membrane, including protonated, hydrogenbonded, and non-hydrogen-bonded water. Protonated water species manifest ${\rm H_3O}^+$ ions, and hydrogen-bonded water molecules refer to those engaged in hydrogen bonding either with each other or with sulfonate groups, whereas non-hydrogen-bonded water molecules are those not participating in hydrogen bonding. Their study revealed that with an increase in RH, the quantity of protonated water species and non-hydrogen-bonded water molecules remains constant, whereas the number of hydrogen-bonded water molecules increases. Consequently, the rise in λ is predominantly attributed to the increase in hydrogen-bonded water molecules, indicating that the clusters and channels consist of water molecules forming the hydrogen bond network, as shown in Fig. 3(d). These hydrogen bonds further

substantiate the intermolecular connections and heat transfer pathways, contributing to the observed thermal conductivity increase.

The same behavior for thermal conductivity increase by water content is also likely to be observed for other PEMs, such as sulfonated polyimide, sulfonated poly(ether ketone ketone), sulfonated poly(ether ether ketone), sulfonated polybenzimidazole, sulfonated polysulfone. It will be of great interest to investigate the effect of water molecules on these PEM structures.

In summary, the out-of-plane thermal conductivity of Nafion was measured under various RH levels, up to 94%, using the DTR technique. The in-plane thermal conductivity was also measured using the TET technique. A comparison of these two thermal conductivities revealed the isotropic structure of the Nafion. Such an exceptional increase in thermal conductivity was observed from 0.110 W m⁻¹ K⁻¹ in vacuum to 0.162 W m⁻¹ K⁻¹ at 16% RH, highlighting the very strong role of water molecules in strengthening the connections between polymer chains. The thermal conductivity further increased to $\sim 0.256\,\mathrm{W\,m^{-1}\,K^{-1}}$ at 70% RH, indicating an enhancement of approximately 60%. Such exceptional increase cannot be explained by the effective medium theory. We attributed this improvement to the water clusters formation within the Nafion structure. The formation of hydrogen bonding among water molecules within clusters creates extra pathways for heat transfer, enhancing thermal conductivity. A maximum thermal conductivity was also observed at this RH (corresponding to $\lambda \approx 6$), attributed to the water channels formation by coalescing water clusters. These channels optimize molecular connections, enhancing thermal pathways efficiently. Thermal conductivity increase with water contents up to $\lambda \approx 6$ shows the Nafion's chemical alteration and hydrogen bonding formation. However, at higher water contents, a negligible increase in thermal conductivity was observed due to water molecules' free movement within established water channels. These channels represent physical changes in Nafion, which have a much smaller impact on thermal conductivity. Furthermore, given that the thermal conductivity of Nafion can vary significantly under different humidity levels, this property suggests that Nafion could be effectively utilized for humidity sensing. This characteristic not only highlights Nafion's potential in sensor applications but also underscores its versatility in environments where precise humidity monitoring is crucial. Additionally, beyond the changes in thermal conductivity and density, other properties such as specific heat, refractive index, and mechanical properties (e.g., Young's modulus and mechanical strength) of Nafion could also be affected due to the improved molecular connections by water molecules.

See the supplementary material for experimental details of outof-plane thermal conductivity measurement, in-plane thermal conductivity measurement, and effective medium theories.

Partial support of this work by the US National Science Foundation (No. CMMI2032464) is gratefully acknowledged.

AUTHOR DECLARATIONS Conflict of Interest

The authors have no conflicts to disclose.

Author Contributions

Mahya Rahbar: Data curation (lead); Formal analysis (lead); Writing – original draft (lead). Qusai Alahmad: Data curation (equal); Formal analysis (equal). John Bai: Data curation (equal); Formal analysis (equal).

Lijun Zhang: Conceptualization (equal); Data curation (equal); Formal analysis (equal); Methodology (equal); Project administration (equal); Writing – review & editing (equal). **Xinwei Wang:** Conceptualization (equal); Data curation (equal); Formal analysis (equal); Funding acquisition (lead); Methodology (lead); Project administration (lead); Resources (lead); Supervision (lead); Writing – review & editing (lead).

DATA AVAILABILITY

The data that support the findings of this study are available from the corresponding authors upon reasonable request.

REFERENCES

- ¹M. Hickner and B. Pivovar, Fuel Cells 5(2), 213 (2005).
- ²H. Nishiyama, S. Takamuku, K. Oshikawa, S. Lacher, A. Iiyama, and J. Inukai, J. Phys. Chem. C **124**(18), 9703 (2020).
- ³K. A. Mauritz and R. B. Moore, Chem. Rev. **104**(10), 4535 (2004).
- O. Burheim, P. Vie, J. Pharoah, and S. Kjelstrup, J. Power Sources 195(1), 249 (2010).
- ⁵M. Khandelwal and M. Mench, J. Power Sources **161**(2), 1106 (2006).
- ⁶N. E. Alhazmi, "Thermal conductivity of proton exchange membrane fuel cell components," Ph.D. thesis (School of Process, Environmental and Materials _Engineering, University of Leeds, 2014).
- ⁷T. A. Zawodzinski, C. Derouin, S. Radzinski, R. J. Sherman, V. T. Smith, T. E. Springer, and S. Gottesfeld, J. Electrochem. Soc. **140**(4), 1041 (1993).
- ⁸P. J. Vie and S. Kjelstrup, Electrochim. Acta **49**(7), 1069 (2004).
- ⁹D. J. Burford and M. M. Mench, in ASME International Mechanical Engineering Congress and Exposition (ASME, 2004), Vol. 4711, p. 317.
- ¹⁰L. Chen, H. Zhang, Z.-Z. Li, Y.-L. He, and W.-Q. Tao, J. Nanosci. Nanotechnol. 15(4), 3087 (2015).
- ¹¹C. Zheng, F. Geng, and Z. Rao, Comput. Mater. Sci. 132, 55 (2017).
- ¹²N. Alhazmi, M. Ismail, D. Ingham, K. Hughes, L. Ma, and M. Pourkashanian, J. Power Sources 241, 136 (2013).
- ¹³N. Alhazmi, D. Ingham, M. Ismail, K. Hughes, L. Ma, and M. Pourkashanian, J. Power Sources 270, 59 (2014).
- ¹⁴O. S. Burheim, ECS Trans. **80**(8), 509 (2017).
- ¹⁵J. Peron, A. Mani, X. Zhao, D. Edwards, M. Adachi, T. Soboleva, Z. Shi, Z. Xie, T. Navessin, and S. Holdcroft, J. Membr. Sci. 356(1-2), 44 (2010).
- ¹⁶Y. Bai, M. S. Schaberg, S. J. Hamrock, Z. Tang, G. Goenaga, A. B. Papandrew, and T. A. Zawodzinski, Jr., Electrochim. Acta 242, 307 (2017).
- ¹⁷C. Feng, Y. Li, K. Qu, Z. Zhang, and P. He, RSC Adv. 9(17), 9594 (2019).
- ¹⁸M. L. Ramires, C. A. Nieto de Castro, Y. Nagasaka, A. Nagashima, M. J. Assael, and W. A. Wakeham, J. Phys. Chem. Ref. Data 24(3), 1377 (1995).
- ¹⁹R. Landauer, J. Appl. Phys. **23**(7), 779 (1952).
- ²⁰R. Davis, Int. J. Thermophys. 7(3), 609 (1986).
- ²¹D. J. Jeffrey, Proc. R. Soc. A **335**, 355–367 (1973).
- ²²F. P. Incropera, D. P. DeWitt, T. L. Bergman, and A. S. Lavine, *Fundamentals of Heat and Mass Transfer* (Wiley, New York, 1996).
- 23 W. Huang, Z. Li, X. Liu, H. Zhao, S. Guo, and Q. Jia, Ann. Glaciol. 54(62), 189 (2013).
- ²⁴P. V. Komarov, P. G. Khalatur, and A. R. Khokhlov, Beilstein J. Nanotechnol. 4(1), 567 (2013).
- 25 L. Zhang, M. Ruesch, X. Zhang, Z. Bai, and L. Liu, RSC Adv. 5(107), 87981 (2015).
- ²⁶T. D. Gierke, G. Munn, and F. Wilson, J. Polym. Sci., Polym. Phys. Ed. **19**(11), 1687 (1981).
- ²⁷W. Y. Hsu and T. D. Gierke, J. Membr. Sci. **13**(3), 307 (1983).
- ²⁸N. Mehra, L. Mu, and J. Zhu, Compos. Sci. Technol. 148, 97 (2017).
- ²⁹Y. Woo, S. Y. Oh, Y. S. Kang, and B. Jung, J. Membr. Sci. **220**(1–2), 31 (2003).
- ³⁰S. Swier, Y. S. Chun, J. Gasa, M. T. Shaw, and R. Weiss, Polym. Eng. Sci. 45(8), 1081 (2005).
- ³¹P. Xing, G. P. Robertson, M. D. Guiver, S. D. Mikhailenko, K. Wang, and S. Kaliaguine, J. Membr. Sci. 229(1–2), 95 (2004).
- ³²J. A. Mader and B. C. Benicewicz, Macromolecules **43**(16), 6706 (2010).
- 33S. Singha, T. Jana, J. A. Modestra, A. N. Kumar, and S. V. Mohan, J. Power Sources 317, 143 (2016).
- ³⁴F. Lufrano, G. Squadrito, A. Patti, and E. Passalacqua, J. Appl. Polym. Sci. 77(6), 1250 (2000).